

A Neutrino Factory for both Large and Small θ_{13}

Alan Bross, Malcolm Ellis, and Steve Geer*

Fermi National Accelerator Laboratory, Batavia, IL 60510-0500, USA

Olga Mena†

INFN - Sez. di Roma, Dipartimento di Fisica, Università di Roma "La Sapienza", P.le A. Moro, 5, I-00185 Roma, Italy

and Silvia Pascoli‡

IPPP, Department of Physics, Durham University, Durham DH1 3LE, United Kingdom

An analysis of the neutrino oscillation physics capability of a low energy Neutrino Factory is presented, including a first simulation of the detector efficiency and event energy threshold. The sensitivity of the physics reach to the presence of backgrounds is also studied. We consider a representative baseline of 1480 km, we use muons with 4.12 GeV energy and we exploit a very conservative estimate of the energy resolution of the detector. Our analysis suggests an impressive physics reach for this setup, which can eliminate degenerate solutions, for both large and small values of the mixing angle θ_{13} , and can determine leptonic CP violation and the neutrino mass hierarchy with extraordinary sensitivity.

PACS numbers: 14.60.Pq

I. INTRODUCTION

In recent years compelling evidence for neutrino oscillations has been found in experiments with atmospheric [1], solar [2, 3, 4, 5, 6, 7], reactor [8] and long-baseline accelerator neutrinos [9, 10]. Two mass squared differences, $\Delta m_{ji}^2 \equiv m_j^2 - m_i^2$, have been measured with good accuracy, their present best fit values being $|\Delta m_{31}^2| = 2.5 \times 10^{-3} \text{ eV}^2$ and $|\Delta m_{21}^2| = 8.0 \times 10^{-5} \text{ eV}^2$. In addition, explaining the experimental data in terms of neutrino oscillations requires two large mixing angles in the leptonic mixing matrix U . Their best fit values are: $\sin^2 \theta_{12} = 0.30$ and $\sin^2 2\theta_{23} = 1$, see Refs. [11, 12, 13]. Despite the remarkable recent progress in our understanding of neutrino physics, fundamental questions remain unanswered. It is crucial to establish the nature of neutrinos - whether they are Dirac or Majorana particles, the neutrino mass ordering, the absolute neutrino mass scale, the value of the unknown mixing angle θ_{13} , the presence or absence of CP violation in the leptonic sector, and the precise values of the already known oscillation parameters. This information will help shed light on the physics beyond the Standard Model responsible for neutrino masses and for the leptonic mixing structure.

In order to achieve these goals, very sensitive neutrino experiments will be required. In particular, long baseline oscillation experiments are expected to play an important role in providing precision measurements of the neutrino oscillation parameters, the CP-violating phase δ , and a determination of the neutrino mass ordering.

Neutrino Factories [14], in which a neutrino beam is generated from muons decaying within the straight sections of a storage ring, have been studied extensively in the past, and have been shown to be sensitive tools for studying neutrino oscillation physics [14, 15, 16, 17, 18, 19, 20, 21, 22, 23, 24]. In a Neutrino Factory far detector, the experimental signature for the so called *golden channel* [18] is the presence of a *wrong-sign* muon [14, 15], i.e. a muon with opposite sign to the muons stored in the neutrino factory. Wrong-sign muons result from $\nu_e \rightarrow \nu_\mu$ oscillations, and can be used

*Electronic address: sgeer@fnal.gov

†Electronic address: omena@fnal.gov

‡Electronic address: silvia.pascoli@durham.ac.uk

to measure the unknown mixing angle θ_{13} , determine the neutrino mass hierarchy, and search for CP violation in the neutrino sector. This physics program requires the detection of charged current (CC) muon-neutrino interactions, and the measurement of the sign of the produced muon. If the interacting neutrinos have energies of more than a few GeV, standard neutrino detector technology, based on large magnetized sampling calorimeters, can be used to measure wrong-sign muons with high efficiency and very low backgrounds. This has been shown to work for Neutrino Factories with energies of about 20 GeV or greater.

Lower energy Neutrino Factories [24], which store muons with energies < 10 GeV, require a detector technology that can detect lower energy muons. Recently ideas have emerged for a Neutrino Factory detector based on a fully active calorimeter within a potentially affordable large volume magnet. These ideas encourage consideration of low energy Neutrino Factories. Initial studies [24], based on a first guess for the performance of a low energy Neutrino Factory detector, suggested that a Neutrino Factory with an energy of about 4 GeV would enable very precise measurements of the neutrino mixing parameters. In the present paper, we consider in more detail the expected performance of a low energy Neutrino Factory detector, and update and extend our previous studies to include a more realistic detector model and a more comprehensive study of systematic effects. In particular we exploit the low energy threshold of the detector and make a very conservative estimate for its energy resolution which, together with the broad spectrum of the neutrino factory beam, facilitates the elimination of degeneracies [25, 26, 27, 28]. It is well known that even a very precise measurement of the appearance probability for neutrinos and antineutrinos at a fixed L/E allows different solutions for $(\theta_{13}, \text{sign}(\Delta m_{13}^2), \delta)$, weakening severely the sensitivity to these parameters. Many strategies have been advocated to resolve this issue which in general involve another detector [19, 29, 30, 31, 32, 33, 34] or the combination with another experiment [22, 23, 35, 36, 37, 38, 39, 40, 41, 42, 43]. Using the energy dependence of the signal in the low energy Neutrino Factory, we find that a 4 GeV Neutrino Factory can unambiguously determine all of the neutrino oscillation parameters with good precision provided $\sin^2 2\theta_{13}$ exceeds the small value of 0.001. Hence a low energy Neutrino Factory would be a precision tool for both large and small θ_{13} .

In Section II we describe the design for the low-threshold detector and its performance. In Section III, we discuss in detail the physics reach of the proposed setup. We first consider the disappearance ν_μ signal in order to determine precisely the value of the atmospheric mass squared difference and, possibly, the type of hierarchy even for $\theta_{13} = 0$. Then, we consider the appearance signals $\nu_e \rightarrow \nu_\mu$ and $\bar{\nu}_e \rightarrow \bar{\nu}_\mu$, which depend on θ_{13} , δ and the type of neutrino mass ordering. We perform a detailed numerical simulation and discuss the sensitivity of the low-energy Neutrino Factory to these parameters. In Section IV, we draw our conclusions.

II. DETECTOR DESIGN AND PERFORMANCE

A totally active scintillator detector (TASD) has been proposed for a Neutrino Factory, and results from a first study of its expected performance are described in the recent International Scoping Study Report [44]. Using a TASD for neutrino physics is not new. Examples are KamLAND [8], which has been operating for several years, and the proposed NO ν A detector [45], which is a 15–18 Kton liquid scintillator detector that will operate off-axis to the NuMI beam line [46] at Fermilab. Note that, unlike KamLAND or NO ν A, the TASD we are investigating for the low energy Neutrino Factory is magnetized and has a segmentation that is approximately 10 times that of NO ν A. Magnetization of such a large volume ($> 30,000 \text{ m}^3$) is the main technical challenge in designing a TASD for a Neutrino Factory, although R&D to reduce the detector cost (driven in part by the large channel count, 7.5×10^6) is also needed.

The Neutrino Factory TASD we are considering consists of long scintillator bars with a triangular cross-section arranged in planes which make x and y measurements (we plan to also consider an x-u-v readout scheme). Optimization of the cell cross section still needs further study since a true triangular cross section results in tracking anomalies at the corners of the triangle. The scintillator bars have a length of 15 m and the triangular cross-section has a base of 3 cm and a height of 1.5 cm. We have considered a design using liquid as in NO ν A, but, compared to NO ν A, the cell size is small (NO ν A uses a $4 \times 6 \text{ cm}^2$ cell) and the non-active component due to the PVC extrusions that hold the liquid becomes quite large (in NO ν A, the scintillator is approximately 70% of the detector mass). Our design is an extrapolation of the MINER ν A experiment [47] which in turn was an extrapolation of the D0 preshower detectors [48]. We are considering a detector mass of approximately 35 Kton (dimensions $15 \times 15 \times 150 \text{ m}$). We believe that an air-core solenoid can produce the field required (0.5 Tesla) to do the physics.

As was mentioned above, magnetizing the large detector volume presents the main technical challenge for a Neutrino Factory TASD. Conventional room temperature magnets are ruled out due to their prohibitive power consumption, and conventional superconducting magnets are believed to be too expensive, due to the cost of the enormous cryostats needed in a conventional superconducting magnet design. In order to eliminate the cryostat, we have investigated a concept based on the superconducting transmission line (STL) that was developed for the Very Large Hadron Collider superfermic magnets [49]. The solenoid windings now consist of this superconducting cable which is confined in its own cryostat (Fig. 1). Each solenoid (10 required for the full detector) consists of 150 turns and requires 7500 m of cable.

There is no large vacuum vessel and thus no large vacuum loads which make the cryostats for large conventional superconducting magnets very expensive. We have performed a simulation [50] of the magnetic cavern concept using STL solenoids and the results are shown in Fig. 2. With the iron end-walls (1 m thick), the average field in the XZ plane is approximately 0.58 T at an excitation current of 50 kA.

The Neutrino Factory TASD response has been simulated using GEANT4 version 8.1 (Fig. 3). The simulated digitization takes into account the dE/dx in the scintillator slabs, and uses a light yield extrapolated from MINER ν A tests. The magnetic field was taken as a uniform 0.5 T field perpendicular to the beam axis. The performance of the detector was studied by simulating the passage of single muons and positrons with a momentum ranging from 100 MeV¹ to 15 GeV. Future studies of this design will include a more realistic field map based on the design work on the magnetic cavern.

The simulated hits were digitized assuming an energy resolution of 2 photo electrons and the reconstruction of clusters imposed a threshold of 0.5 photo electrons before building space points and performing a track fit using the Kalman Fitting package RecPack [51].

In order to study the momentum resolution and the rate at which the charge of a muon is mis-identified, 2.3 million muons were simulated, of which, 1.8 million, divided equally in two uniformly populated momentum ranges (0.1 – 1 GeV and 1 – 10 GeV), were analyzed. The position resolution was found to be approximately 4.5 mm RMS with a central Gaussian with width of 2.5 mm². The momentum resolution as a function of the muon momentum is shown in Fig. 4. The tracker achieves a resolution of better than 10% over the complete momentum range studied. Due to the low density of the TASD, it is possible to reconstruct muons down to a few hundred MeV. Figure 5(a) shows the efficiency for reconstructing positive muons as a function of the initial momentum of the muon. The detector becomes fully efficient above 400 MeV.

The charge of the muon was determined by performing two separate Kalman track fits, one with a positive charge and the other with a negative charge. The charge mis-identification rate was determined by counting the rate at which the track fit with the incorrect charge resulted in a better χ^2 per degree of freedom. Figure 5(b) shows the charge mis-identification rate as a function of the initial muon momentum.

Using the NUANCE [52] event generator, 1 million ν_e and 1 million ν_μ events were generated in 50 mono-energetic neutrino energy bins between 100 MeV and 5 GeV. The results shown below, however, only have one thousand events processed through the GEANT4 simulation. For this analysis pattern recognition had not yet been implemented. Monte Carlo information was used to group hits by the particle that produced them and every fourth hit is used as a space point (gaussian smeared with a 4.5 mm resolution) and passed to a Kalman track fit routine. At this time the Kalman fit does not incorporate multiple Coulomb scattering or dE/dx corrections. A minimum of 10 points were required in order to perform the track fit. The reconstruction returned:

- the total momentum vector of all fitted tracks,
- the momentum vector of the muon (muon ID from MC truth),
- the reconstructed and truth energy sum of all the hits that were not in a particle that was fitted, and
- the reconstructed energy sum of all hits in the event.

The ν_μ CC event reconstruction efficiency as a function of neutrino energy is shown in Fig. 6(a). The fraction of ν_μ CC events with a reconstructed muon is shown in Fig. 6(b). In this figure the bands represent the limits of the statistical errors for this analysis.

Based on these initial Neutrino Factory TASD studies, in our phenomenological analysis we assume the detector has an effective threshold for measuring muon neutrino CC events at $E_\nu = 500$ MeV, above which it has an energy independent efficiency of 73%. The 73% efficiency is primarily driven by the neutrino interaction kinematics, not by the detector tracking efficiency. No charge-ID criterion is applied here. The charge misidentification rate information is used as input into the effect of backgrounds on the analysis.

III. PHYSICS REACH OF THE LOW ENERGY NEUTRINO FACTORY

We have previously mentioned that, by exploiting the energy dependence of the signal, it is possible to extract from the measurements the correct values of θ_{13} and δ , and eliminate the additional solutions arising from discrete

¹ In the present article, we use natural units for which $c = 1$.

² At this stage, the simulation does not take into account light collection inefficiencies in the corners of the base of the triangle.

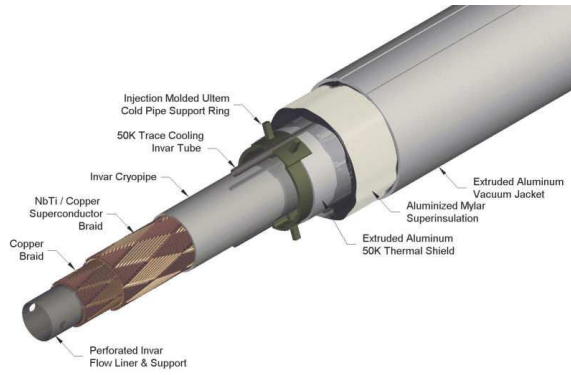


FIG. 1: *Diagram of Superconducting Transmission Line design.*

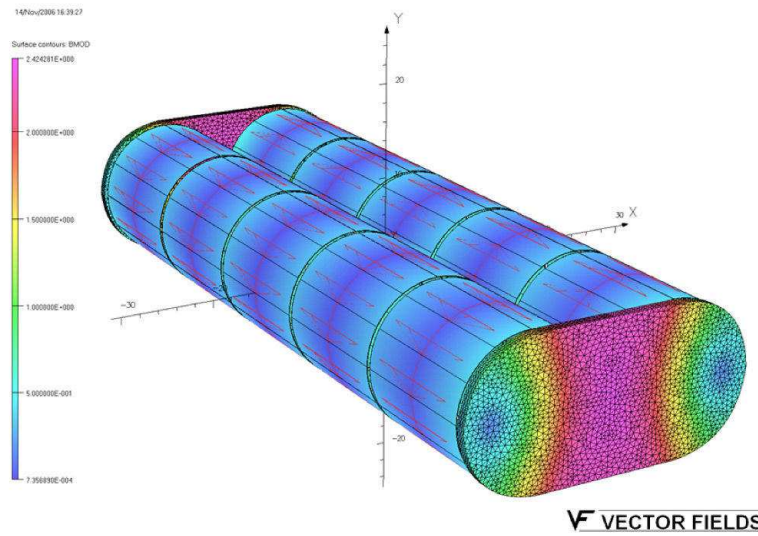


FIG. 2: *Simulation results for magnetic cavern design.*

ambiguities. In the present study, we include the detector simulation results described in the previous section, which suggests a lower energy threshold (500 MeV) than previously assumed [24], and an energy resolution $dE/E = 30\%$ ³. Above threshold, the detector efficiency for muon neutrino CC events is taken to be 73%.

In the following we consider the representative baseline $L = 1480$ km, which corresponds to the distance from Fermilab to the Henderson mine. However, we believe that the TASD will not require operation deep underground in order to remove backgrounds. Results are similar for other baselines in the 1200–1500 km range. The results are presented for both the low- and high-statistics scenarios described in [24]. The low-statistics scenario corresponds to 3×10^{22} Kton-decays (5 years of data taking with 3×10^{20} useful muon decays of each sign per year, and a detector fiducial mass times efficiency of 20 Kt). The high-statistics scenario corresponds to 1×10^{23} Kton-decays (10 years of data taking, with 5×10^{20} useful muon decays of each sign per year, and a detector fiducial mass times efficiency of 20 Kt). Table I shows the number of CC muon events expected in both the low- and high-statistics scenarios for, respectively, the positive and negative muons stored in the Neutrino Factory. Even in the low statistics case, in the absence of oscillations there would be a few times 10^4 ν_e CC interactions, which would allow a search for $\nu_e \rightarrow \nu_\mu$ oscillations with probabilities below 10^{-4} .

³ We have assumed a very conservative $dE/E = 30\%$ because at this time the simulation work has not yet produced a number for the TASD. Based on NO ν A results, we expect the TASD dE/E to be better than 6% at 2 GeV.

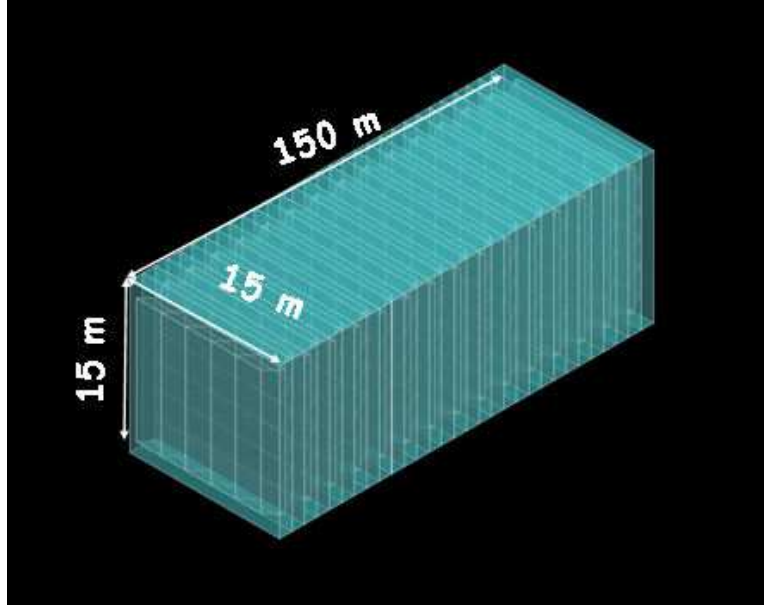


FIG. 3: Schematic of Totally Active Scintillator Detector.

$E_{\mu^\pm} =$ 4.12 GeV		μ^+		μ^-	
		$N_{\bar{\nu}_\mu}/10^3$	$N_{\nu_e}/10^3$	$N_{\nu_\mu}/10^3$	$N_{\bar{\nu}_e}/10^3$
statistics	3	39	66	77	34
(10^{22}) Kt-decays	10	131	220	257	112

TABLE I: Neutrino and antineutrino charged currents interaction rates for $L = 1480$ km, for the low- and high-statistics cases, which correspond respectively to 3×10^{22} and 1×10^{23} Kt-decays.

All numerical results reported in the next subsections have been obtained with the exact formulae for the oscillation probabilities. Unless specified otherwise, we take the following central values for the remaining oscillation parameters: $\sin^2 \theta_{12} = 0.29$, $\Delta m_{21}^2 = 8 \times 10^{-5} \text{ eV}^2$, $|\Delta m_{31}^2| = 2.5 \times 10^{-3} \text{ eV}^2$ and $\theta_{23} = 40^\circ$. We show in Tables II and III, for two representative values of $\theta_{13} = 1^\circ$ and 8° , and the CP phase $\delta = 0^\circ, 90^\circ, 180^\circ$ and 270° , the number of *wrong-sign* muon events in the low- and high-statistics scenarios for, respectively, the positive and negative muons stored in the Neutrino Factory, for normal (inverted) hierarchy.

statistics (Kt-decays)	$\delta(^{\circ})$	μ^+ stored (wrong-sign: μ^-)	μ^- stored (wrong-sign: μ^+)
3×10^{22}	0	2640 (1020)	540 (1550)
	90	3700 (1520)	270 (990)
	180	2990 (1020)	510 (1310)
	270	1930 (520)	780 (1870)
1×10^{23}	0	8830 (3400)	1800 (5170)
	90	12330 (5070)	900 (3300)
	180	9970 (3400)	1700 (4370)
	270	6430 (1730)	2600 (6240)

TABLE II: Wrong sign muon event rates for normal (inverted) hierarchy, assuming $\nu_e \rightarrow \nu_\mu$ ($\bar{\nu}_e \rightarrow \bar{\nu}_\mu$) oscillations in a 20 Kt fiducial volume detector, for a $L = 1480$ km baseline. We assume here $\theta_{13} = 8^\circ$, i.e. $\sin^2 2\theta_{13} \simeq 0.076$. We present the results for several possible values of the CP-violating phase δ for both the low and the high luminosity scenario.

For our analysis, we use the following χ^2 definition

$$\chi^2 = \sum_{i,j} \sum_{p,p'} (n_{i,p} - N_{i,p}) C_{i,p;j,p'}^{-1} (n_{j,p'} - N_{j,p'}), \quad (3.1)$$

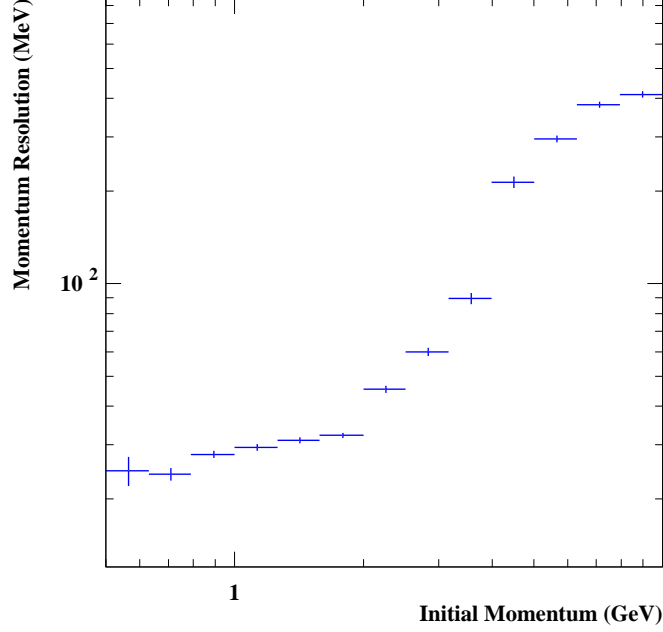


FIG. 4: *Momentum resolution as a function of the muon momentum.*

statistics (Kt-decays)	$\delta(^{\circ})$	μ^{+} stored (wrong-sign: μ^{-})	μ^{-} stored (wrong-sign: μ^{+})
3×10^{22}	0	160 (150)	80 (110)
	90	300 (210)	40 (30)
	180	200 (150)	70 (75)
	270	65 (90)	110 (150)
1×10^{23}	0	530 (500)	270 (370)
	90	1000 (700)	130 (100)
	180	670 (500)	230 (250)
	270	220 (300)	370 (500)

TABLE III: *As Table II but for $\theta_{13} = 1^{\circ}$, i.e. $\sin^2 2\theta_{13} \simeq 0.001$.*

where $N_{i,\pm}^{\lambda}$ is the predicted number of muons for a certain oscillation hypothesis, $n_{i,p}$ are the simulated “data” from a Gaussian or Poisson smearing and C is the $2N_{bin} \times 2N_{bin}$ covariance matrix given by:

$$C_{i,p;j,p'}^{-1} \equiv \delta_{ij}\delta_{pp'}(\delta n_{i,p})^2 \quad (3.2)$$

where $(\delta n_{i,p}) = \sqrt{n_{i,p} + (f_{sys} \cdot n_{i,p})^2}$ contains both statistical and a 2% overall systematic error ($f_{sys} = 0.02$). The C.L. contour plots presented in the figures have been calculated for 2 d.o.f..

A. Exploring the disappearance channel

Consider first the disappearance channels, already considered in the context of Neutrino Factories [17, 53] and carefully explored in Ref. [54]. In Ref. [24] it was shown that, with its high statistics and good energy resolution, a low energy neutrino factory can be used to precisely determine the atmospheric neutrino oscillation parameters, θ_{23} and Δm_{31}^2 . In particular, for an exposure of 3×10^{22} Kton-decays for each muon sign, and allowing for a 2% systematic uncertainty, it was shown that: (i) Maximal mixing in the 23-sector could be excluded at 99% CL if

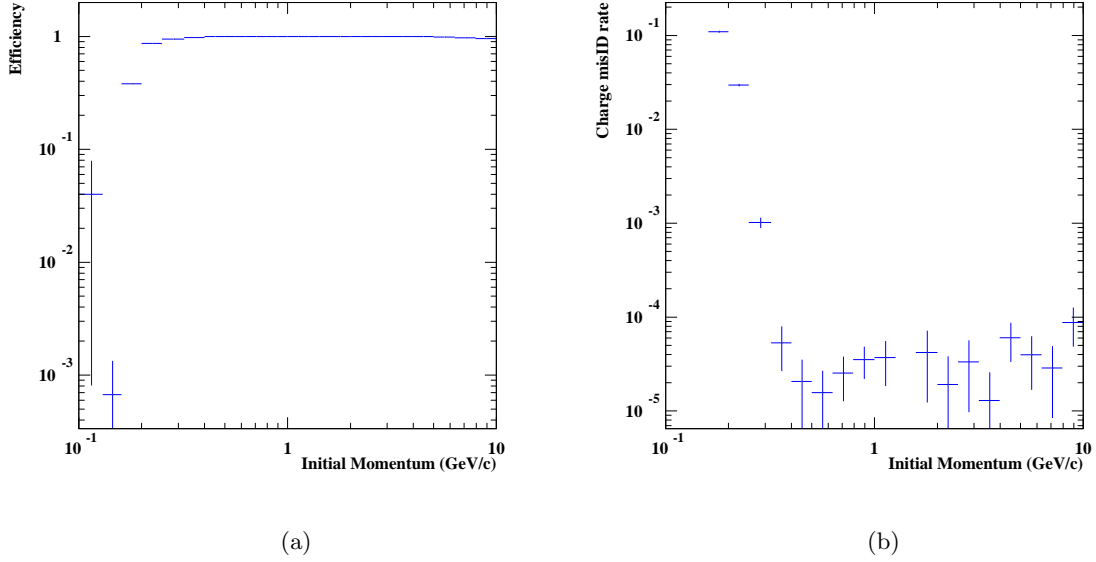


FIG. 5: (a) Efficiency for reconstructing positive muons. (b) Muon charge mis-identification rate as a function of the initial muon momentum.

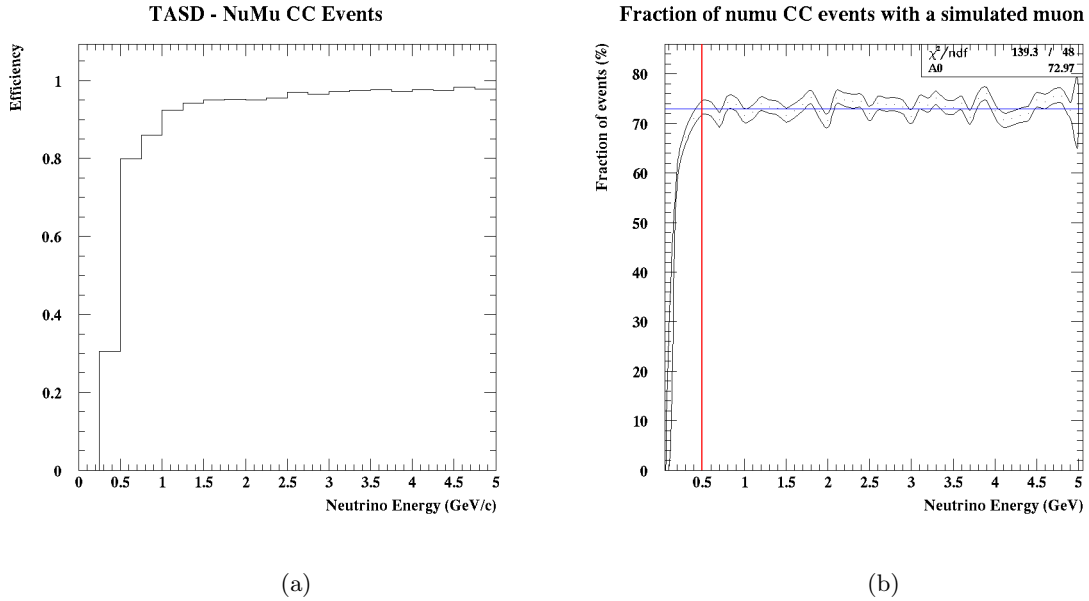


FIG. 6: (a) Reconstruction efficiency of NuMu CC events as a function of neutrino interaction energy. (b) Fraction of NuMu CC events with a reconstructed muon.

$\sin^2 \theta_{23} < 0.48$ ($\theta_{23} < 43.8^\circ$), independently of the value of θ_{13} , and (ii) For a large value of θ_{13} , i.e. $\theta_{13} > 8^\circ$, the θ_{23} -octant degeneracy would be resolved at the 99% CL for $\sin^2 \theta_{23} < 0.44$ ($\theta_{23} < 41.5^\circ$). In our present study, the good energy resolution of the TASD provides sensitivity to the oscillatory pattern of the disappearance signal that is comparable to, and somewhat better than, we previously assumed. In Fig. 7 we show the 90%, 95% and 99% CL contours (for 2 d.o.f) resulting from the fits to the measured energy dependent ν_μ and $\bar{\nu}_\mu$ CC rates at $L = 1480$ km. Results correspond to 3×10^{22} Kton-decays, and are shown for $\Delta m_{31}^2 = 2.5 \times 10^{-3} \text{ eV}^2$ and two simulated values of $\sin^2 \theta_{23}$ ($= 0.4$ and 0.44). For $\theta_{13} = 0$, $P_{\nu_\mu \rightarrow \nu_\mu}(\theta_{23}) = P_{\nu_\mu \rightarrow \nu_\mu}(\pi/2 - \theta_{23})$, i.e. the disappearance channel is symmetric under $\theta_{23} \rightarrow \pi/2 - \theta_{23}$. However, when a rather large non-vanishing value of θ_{13} is switched on, a θ_{23} asymmetry

appears in the $P_{\nu_\mu \rightarrow \nu_\mu}$. Notice that the asymmetry grows with increasing θ_{13} and the four-fold degeneracy in the atmospheric neutrino parameters is solved more easily. We conclude that, using only the ν_μ -disappearance data, the uncertainty on Δm_{31}^2 could be reduced down to the 1% – 2% level. In principle, the ν_e disappearance channel could also be used, which is sensitive to θ_{13} and matter effects. However, charge discrimination for electrons has not yet been adequately studied to determine the relevant TASD performance parameters.

The extremely good determination of the atmospheric mass squared difference opens the possibility to determine the mass hierarchy by exploiting the effects of the solar mass squared difference on the ν_μ disappearance probability, even for negligible values of θ_{13} . This strategy was studied in detail in Refs. [55, 56, 57]. The vacuum $\nu_\mu \rightarrow \nu_\mu$ oscillation probability is given by

$$P(\nu_\mu \rightarrow \nu_\mu) = 1 - 4|U_{\mu 1}|^2|U_{\mu 2}|^2 \sin^2 \frac{\Delta m_{12}^2 L}{4E} - 4|U_{\mu 1}|^2|U_{\mu 3}|^2 \sin^2 \frac{\Delta m_{13}^2 L}{4E} - 4|U_{\mu 2}|^2|U_{\mu 3}|^2 \sin^2 \frac{\Delta m_{23}^2 L}{4E}, \quad (3.3)$$

where the usual notation is used for the mass squared differences Δm_{ij}^2 and for the elements of the leptonic mixing matrix U . In the following we take $\theta_{13} = 0$. The oscillation probabilities depend on whether $|\Delta m_{13}^2| > |\Delta m_{23}^2|$ (normal hierarchy) or $|\Delta m_{13}^2| < |\Delta m_{23}^2|$ (inverted hierarchy). Precisely measured disappearance probabilities can distinguish between normal and inverted hierarchies if there is sensitivity to effects driven by both $|\Delta m_{13}^2|$ and Δm_{12}^2 . This requires the atmospheric mass squared difference to be measured at different L/E with a precision of better than $|\Delta m_{21}^2|/|\Delta m_{31}^2| \sim 0.026$. In fact, it was pointed out in Ref. [55] that, for a fixed L/E , the disappearance probabilities for the normal and inverted hierarchies are the same if $|\Delta m_{13}^2|$ is substituted with $-|\Delta m_{13}^2| + \Delta m_{12}^2 + \frac{4E}{L} \arctan\left(\cos 2\theta_{12} \tan \frac{\Delta m_{12}^2 L}{4E}\right)$. In order to break this degeneracy it is necessary to measure the atmospheric mass squared difference at different energies and at distances for which the oscillations driven by the solar term are non negligible. In our setup, if we assume a 0% (2%) overall systematic error, we find that the hierarchy can be resolved at 90% C.L. (cannot be resolved) for the low statistics case, while for the high statistics scenario it can be determined at 95% C.L. (90% C.L.). Note that the systematic errors play a crucial role. It is in principle possible to reduce the impact of the systematics errors using the ratios of the number of events at the near and far detectors:

$$\mathcal{R}(E) = \frac{\frac{N_N(\nu_\mu)}{N_N(\bar{\nu}_e)}}{\frac{N_F(\nu_\mu)}{N_F(\bar{\nu}_e)}}, \quad (3.4)$$

where $N_{N(F)}(\nu_\mu[\bar{\nu}_e])$ refer to the number of ν_μ [$\bar{\nu}_e$] events in the near (far) detector for a fixed energy E . Very good energy resolution is required for such cancellations to be effective. In this case, a low energy Neutrino Factory can give important information on the type of hierarchy even if $\theta_{13} = 0$.

B. Simultaneous fits to θ_{13} and δ

Next, we study the extraction of the unknown parameters θ_{13} and δ , using the *golden channel* ($\nu_e(\bar{\nu}_e) \rightarrow \nu_\mu(\bar{\nu}_\mu)$). We start by considering the low statistics neutrino factory scenario with 3×10^{22} Kton-decays. We find that, for values of $\theta_{13} > 2^\circ$, the sign degeneracy is resolved at the 99% CL and the θ_{23} octant degeneracy is solved at the 95% CL. Note that for $\theta_{13} > 4^\circ$ the octant degeneracy has already been resolved using the disappearance data.

Figure 8 shows, for a fit to the simulated data at a baseline $L = 1480$ km, the 90%, 95% and 99% CL contours in the (θ_{13}, δ) -plane. Results are shown for background levels set to zero (left panel) and 10^{-3} (right panel). The four sets of contours correspond to four simulated test points in the (θ_{13}, δ) -plane, which are depicted by a star. The simulations are for the normal mass hierarchy and θ_{23} in the first octant ($\sin^2 \theta_{23} = 0.41$ which corresponds to $\theta_{23} = 40^\circ$). Our analysis includes the study of the discrete degeneracies. That is, we have fitted the data assuming both the right and wrong hierarchies, and the right and wrong choices for the θ_{23} octant. If present, the additional solutions associated to the θ_{23} octant ambiguity are shown as dotted contours. Notice from Fig. 8 that the sign ambiguity is solved at the 99% CL. The additional solutions associated to the wrong choice of the θ_{23} octant are present at the 95% and at the 99% CL, but notice that the presence of these additional solutions does not interfere with a measurement of the CP violating phase δ and θ_{13} , since the locations of the fake solutions in the (θ_{13}, δ) plane, are almost the same as the correct locations.

We illustrate the corresponding results for the high statistics scenario in Fig. 9. Note that the higher statistics allows us to consider a smaller value for $\theta_{13} = 1^\circ$. The additional solutions arising from the wrong choice for the neutrino mass hierarchy or θ_{23} octant are not present at the 99% CL. Furthermore, the addition of a background level of 10^{-3} does not significantly affect the resolution of the degeneracies, and has only an impact on the CP violation measurement. The effect of the background can be easily understood in terms of the statistics presented in Tables II

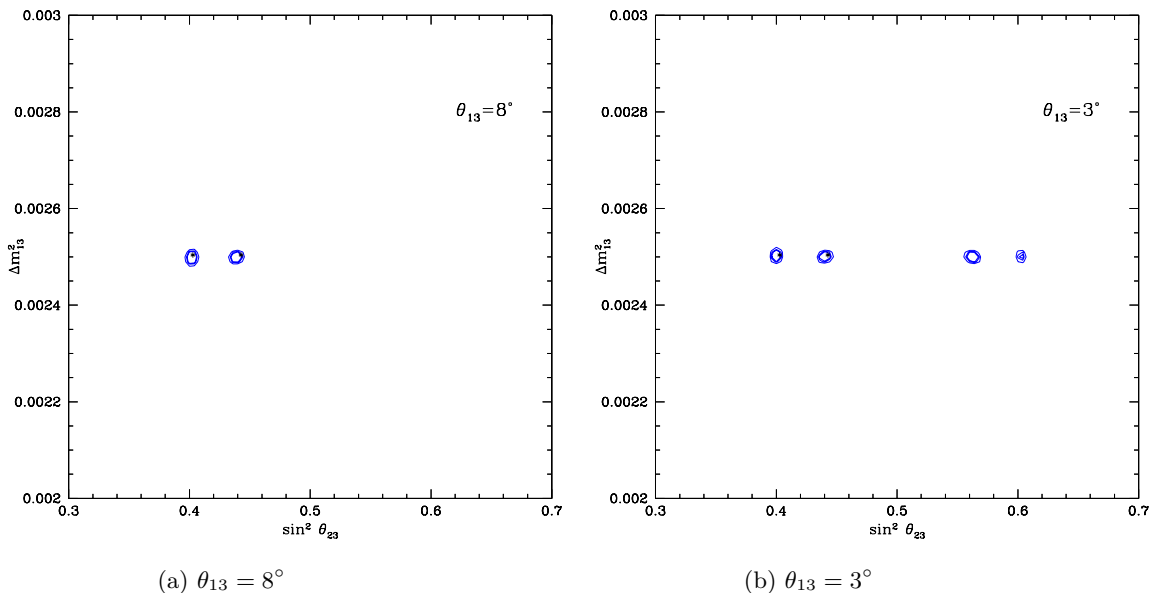


FIG. 7: 90%, 95% and 99% (2 d.o.f) CL contours resulting from the fits at $L = 1480$ km assuming two central values for $\sin^2 \theta_{23} = 0.4$ and 0.44 and $\Delta m_{31}^2 = 2.5 \times 10^{-3} \text{ eV}^2$. In the left (right) panel, $\theta_{13} = 8^\circ$ (3°). The statistics considered for both simulations corresponds to 3×10^{22} Kton-decays. Only disappearance data have been used to perform these plots.

and III. For small values of θ_{13} , the addition of the background has a larger impact for $\delta \sim -90^\circ$, since for that value of the CP phase the statistics are dominated by the antineutrino channel, which suffers from a larger background (from ν_μ 's) than the neutrino channel (from $\bar{\nu}_\mu$'s). For a background level smaller than $\sim 10^{-4}$, the results are indistinguishable from the zero background case.

The performance of the *low energy neutrino factory*, even in the low statistics scenario and with a 10^{-3} background fraction, is unique. With a 10^{-3} background level, the $\text{sign}(\Delta m_{31}^2)$ can be determined at the 99% CL in the low (high) statistics scenario if $\theta_{13} > 2^\circ$ ($> 1^\circ$) for all values of the CP phase δ . The θ_{23} -octant ambiguity can be removed at the 99% CL down to roughly $\theta_{13} > 0.5^\circ$ ($> 0.3^\circ$) for the representative choice of $\sin^2 \theta_{23} = 0.41$, independently of the value of δ , except for some intermediate values of $\theta_{13} \sim 2^\circ$, for which the θ_{23} degeneracy could be resolved at the 95% CL. Solving the θ_{23} -octant degeneracy therefore is easier for small values of $\theta_{13} < 2^\circ$. This is due to the fact that, as explored in Ref. [24], the θ_{23} -octant degeneracy is solved using the information from the low energy bins, which are sensitive to the solar term. For the setup described in this paper, the solar term starts to be important if $\theta_{13} < 2^\circ$.

In Figs. 10 and 11 we summarize, for the low- and high-statistics cases, the physics reach for a TASD detector located 1480 km from a low energy neutrino factory. The analysis takes into account the impact of both the intrinsic and discrete degeneracies. Figure 10 shows the region in the $(\sin^2 2\theta_{13}, \text{"fraction of } \delta\text{"})$ plane for which the mass hierarchy can be resolved at the 99% CL(2 d.o.f). Contours are shown for zero background, and for when a background level of 10^{-3} is included in the analysis. Note that, with a background level of $\simeq 10^{-3}$, the hierarchy can be determined in both low- and high-statistics scenarios if $\sin^2 2\theta_{13} > 0.004$ (i.e. $\theta_{13} > 2^\circ$) for all values of the CP violating phase δ .

Figure 11 shows the region in the $(\sin^2 2\theta_{13}, \delta)$ plane for which a given (non-zero) CP violating value of the CP-phase δ can be distinguished at the 99% CL (2 d.o.f.) from the CP conserving case, i.e. $\delta = 0, \pm 180^\circ$. The results are given for both the low- and high-statistics scenarios. Note that, even in the presence of a 10^{-3} background level, the CP violating phase δ could be measured with a 99% CL precision of better than 20° in the low (high) luminosity scenario if $\sin^2 2\theta_{13} > 0.004$ ($\sin^2 2\theta_{13} > 0.001$).

IV. SUMMARY AND CONCLUSIONS

We have studied the physics reach of a *low energy neutrino factory*, first presented in Ref. [24], in which the stored muons have an energy of 4.12 GeV. The simulated detector performance is based upon a magnetized Totally Active Scintillator Detector. Our simulations suggest this detector will have a threshold for measuring muon neutrino CC interactions of about 500 MeV and an energy independent efficiency of about 73% above threshold. We have assumed

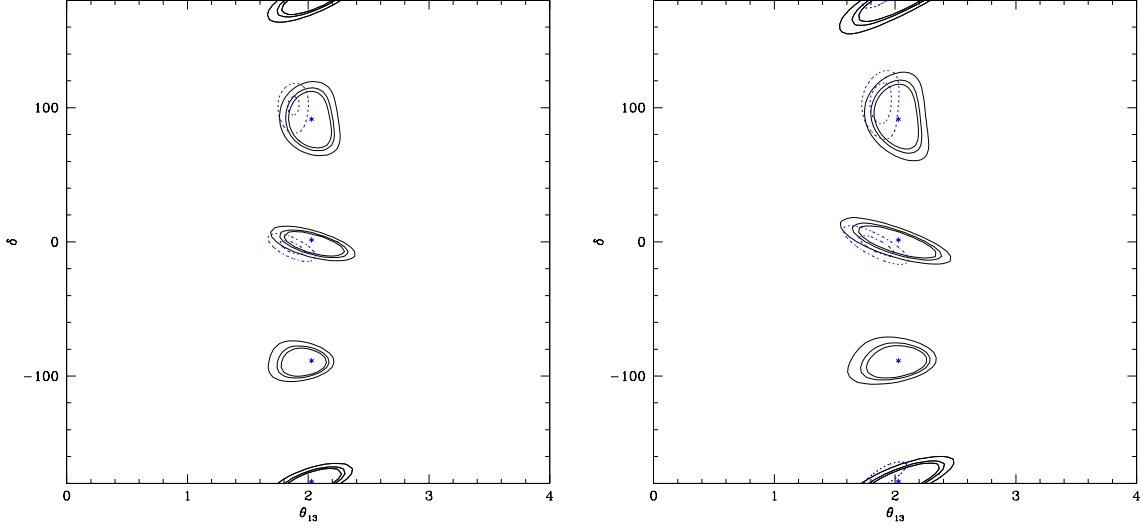


FIG. 8: 90%, 95% and 99% (2 d.o.f) CL contours resulting from the fits at $L = 1480$ km assuming four central values for $\delta = 0^\circ, 90^\circ, -90^\circ$ and 180° and $\theta_{13} = 2^\circ$ without backgrounds (left panel) and with a background level of 10^{-3} (right panel). The additional θ_{23} octant solutions are depicted in dotted blue. The statistics considered for both simulations corresponds to 3×10^{22} Kton-decays.

a conservative energy resolution of 30% for the detector.

In our analysis, we consider the representative baseline of 1480 Km, divide the simulated observed neutrino event spectrum into 9 energy bins above the 500 MeV threshold, and exploit both the disappearance ($\nu_\mu \rightarrow \nu_\mu$) and the *golden* ($\nu_e \rightarrow \nu_\mu$) channels by measuring CC events tagged by “right-sign” and “wrong-sign” muons. The results can be easily generalized to other baselines in the 1200–1500 km range. We have investigated the dependence of the physics sensitivity on statistics by considering a low statistics scenario corresponding to 3×10^{22} Kt-decays for each muon sign, and a high statistics scenario corresponding to 1×10^{23} Kt-decays for each muon sign. We have also explored the impact of backgrounds to the wrong-sign muon signal by considering background levels of zero and 10^{-3} .

We find that, based only on the disappearance channel, maximal atmospheric neutrino mixing can be excluded at 99% CL if $\sin^2 \theta_{23} < 0.48$ ($\theta_{23} < 43.8^\circ$). The atmospheric mass difference could be measured with a precision of 1% – 2%, opening the possibility of determining the neutrino mass hierarchy even if $\theta_{13} = 0$ provided systematic uncertainties can be controlled. Neglecting systematic uncertainties, the mass hierarchy could be determined at the 90% CL (95% CL) in the low (high) statistics scenario.

The rich oscillation pattern of the $\nu_e \rightarrow \nu_\mu$ ($\bar{\nu}_e \rightarrow \bar{\nu}_\mu$) appearance channels at energies between 0.5 and 4 GeV for baselines $\mathcal{O}(1000)$ km facilitates an elimination of the degenerate solutions. If the atmospheric mixing angle is not maximal, for the representative choice of $\sin^2 \theta_{23} = 0.4$, the octant in which θ_{23} lies could be extracted at the 99% CL in the low (high) statistics scenarios if $\theta_{13} > 0.5^\circ$ ($\theta_{13} > 0.3^\circ$), for all values of the CP violating phase δ .

In the low statistics scenario, if the background level is $\sim 10^{-3}$ (10^{-4}), the neutrino mass hierarchy could be determined at the 99% CL, and the CP violating phase δ could be measured with a 99% CL precision of better than 20° , if $\sin^2 2\theta_{13} > 0.005$ (0.002). The corresponding numbers for the high statistics scenario are $\sin^2 2\theta_{13} = 0.001$ and $\sin^2 2\theta_{13} = 0.0003$, for background levels of 10^{-3} and 10^{-4} , respectively. In our analysis we have included a 2% systematic error on all measured event rates.

In summary, the low statistics low energy Neutrino Factory scenario we have described, with a background level of 10^{-3} , for both large and very small values of θ_{13} would be able to eliminate ambiguous solutions, determine θ_{13} , the mass hierarchy, and search for CP violation. Higher statistics and lower backgrounds would further improve the sensitivity, and may enable the mass hierarchy to be determined even if $\theta_{13} = 0$.

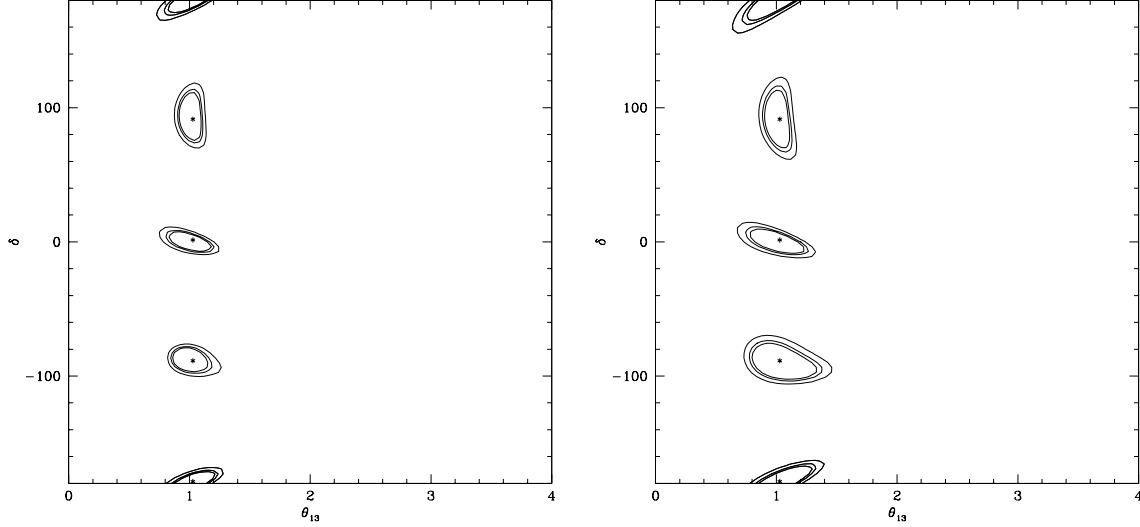


FIG. 9: 90%, 95% and 99% (2 d.o.f) CL contours resulting from the fits at $L = 1480$ km assuming four central values for $\delta = 0^\circ, 90^\circ, -90^\circ$ and 180° and $\theta_{13} = 1^\circ$ without backgrounds (left panel) and with a background level of 10^{-3} (right panel). The statistics considered for both simulations corresponds to 1×10^{23} Kton-decays.

Acknowledgments

This work was supported in part by the European Programme “The Quest for Unification” contract MRTN-CT-2004-503369, and by the Fermi National Accelerator Laboratory, which is operated by the Fermi Research Association, under contract No. DE-AC02-76CH03000 with the U.S. Department of Energy. SP acknowledges the support of CARE, contract number RII3-CT-2003-506395. OM and SP would like to thank the Theoretical Physics Department at Fermilab for hospitality and support.

-
- [1] Y. Ashie *et al.* [Super-Kamiokande Collaboration], Phys. Rev. D **71**, 112005 (2005).
 - [2] B. T. Cleveland *et al.*, Astrophys. J. **496**, 505 (1998); Y. Fukuda *et al.* [Kamiokande Collaboration], Phys. Rev. Lett. **77**, 1683 (1996); J. N. Abdurashitov *et al.* [SAGE Collaboration], J. Exp. Theor. Phys. **95**, 181 (2002); W. Hampel *et al.* [GALLEX Collaboration], Phys. Lett. B **447**, 127 (1999); T. A. Kirsten [GNO Collaboration], Nucl. Phys. Proc. Suppl. **118**, 33 (2003).
 - [3] S. Fukuda *et al.* [Super-Kamiokande Collaboration], Phys. Lett. B **539**, 179 (2002).
 - [4] Q. R. Ahmad *et al.* [SNO Collaboration], Phys. Rev. Lett. **87**, 071301 (2001).
 - [5] Q. R. Ahmad *et al.* [SNO Collaboration], Phys. Rev. Lett. **89**, 011301 (2002) and *ibid.* **89**, 011302 (2002).
 - [6] S. N. Ahmed *et al.* [SNO Collaboration], Phys. Rev. Lett. **92**, 181301 (2004).
 - [7] B. Aharmim *et al.* [SNO Collaboration], Phys. Rev. C **72**, 055502 (2005).
 - [8] K. Eguchi *et al.* [KamLAND Collaboration], Phys. Rev. Lett. **90**, 021802 (2003).
 - [9] M. H. Ahn *et al.* [K2K Collaboration], Phys. Rev. D **74**, 072003 (2006).
 - [10] D. G. Michael *et al.* [MINOS Collaboration], Phys. Rev. Lett. **97**, 191801 (2006).
 - [11] T. Schwetz, Phys. Scripta **T127**, 1 (2006).
 - [12] G. L. Fogli *et al.*, Phys. Rev. D **75**, 053001 (2007).
 - [13] M. C. Gonzalez-Garcia and M. Maltoni, arXiv:0704.1800 [hep-ph].
 - [14] S. Geer, Phys. Rev. D **57**, 6989 (1998) [Erratum-*ibid.* D **59**, 039903 (1999)].
 - [15] A. De Rujula, M. B. Gavela and P. Hernandez, Nucl. Phys. B **547**, 21 (1999).
 - [16] V. D. Barger, S. Geer and K. Whisnant, Phys. Rev. D **61**, 053004 (2000); A. Donini *et al.*, Nucl. Phys. B **574**, 23 (2000); V. D. Barger *et al.*, Phys. Rev. D **62**, 073002 (2000).
 - [17] V. D. Barger *et al.*, Phys. Rev. D **62**, 013004 (2000).
 - [18] A. Cervera, *et al.* Nucl. Phys. B **579**, 17 (2000) [Erratum-*ibid.* B **593**, 731 (2001)]; M. Freund, P. Huber and M. Lindner, Nucl. Phys. B **585**, 105 (2000); V. D. Barger *et al.*, Phys. Lett. B **485**, 379 (2000); J. Burguet-Castell *et al.*, Nucl. Phys. B

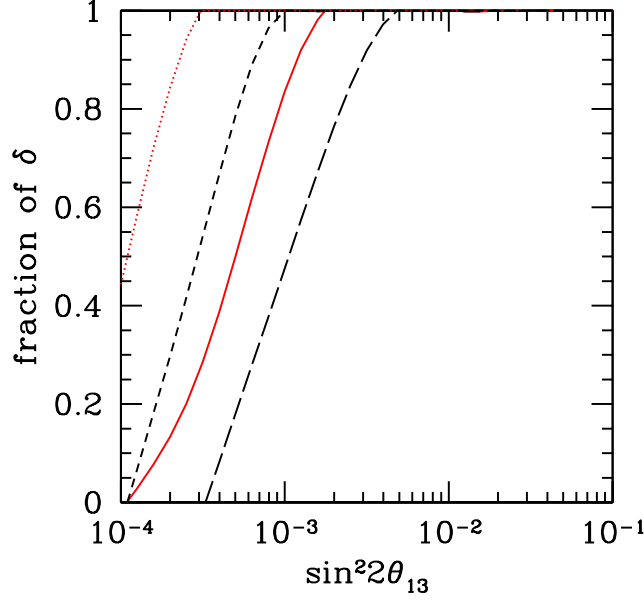


FIG. 10: 99% *CL* hierarchy resolution (2 d.o.f) assuming that the far detector is located at a distance of 1480 km at the Henderson mine. The solid (dotted) red curves depict the results assuming 3×10^{22} Kton-decays (1×10^{23} Kton-decays) without backgrounds. The long-dashed (short-dashed) black curves depict the results assuming 3×10^{22} Kton-decays (1×10^{23} Kton-decays) with a background level of 10^{-3} .

- 608**, 301 (2001); M. Freund, P. Huber and M. Lindner, Nucl. Phys. B **615**, 331 (2001).
- [19] A. Donini, D. Meloni and P. Migliozzi, Nucl. Phys. B **646**, 321 (2002);
D. Autiero *et al.*, Eur. Phys. J. C **33**, 243 (2004).
- [20] C. Albright *et al.*, arXiv:hep-ex/0008064.
- [21] A. Blondel *et al.*, Nucl. Instrum. Meth. A **451**, 102 (2000);
M. Apollonio *et al.*, arXiv:hep-ph/0210192;
C. Albright *et al.* [Neutrino Factory/Muon Collider Collaboration], arXiv:physics/0411123.
- [22] O. Mena, Mod. Phys. Lett. A **20**, 1 (2005).
- [23] P. Huber, M. Lindner, M. Rolinec and W. Winter, Phys. Rev. D **74**, 073003 (2006).
- [24] S. Geer, O. Mena and S. Pascoli, Phys. Rev. D **75**, 093001 (2007).
- [25] G. L. Fogli and E. Lisi, Phys. Rev. D **54**, 3667 (1996).
- [26] H. Minakata and H. Nunokawa, JHEP **0110**, 001 (2001).
- [27] V. D. Barger, S. Geer, R. Raja and K. Whisnant, Phys. Rev. D **63**, 113011 (2001).
- [28] T. Kajita, H. Minakata and H. Nunokawa, Phys. Lett. B **528**, 245 (2002); H. Minakata, H. Nunokawa and S. J. Parke, Phys. Rev. D **66**, 093012 (2002); P. Huber, M. Lindner and W. Winter, Nucl. Phys. B **645**, 3 (2002); A. Donini, D. Meloni and S. Rigolin, JHEP **0406**, 011 (2004); M. Aoki, K. Hagiwara and N. Okamura, Phys. Lett. B **606**, 371 (2005); O. Yasuda, New J. Phys. **6**, 83 (2004); O. Mena and S. J. Parke, Phys. Rev. D **72**, 053003 (2005).
- [29] H. Minakata and H. Nunokawa, Phys. Lett. B **413**, 369 (1997).
- [30] V. Barger, D. Marfatia and K. Whisnant, Phys. Rev. D **66**, 053007 (2002).
- [31] O. Mena Requejo, S. Palomares-Ruiz and S. Pascoli, Phys. Rev. D **72**, 053002 (2005).
- [32] M. Ishitsuka *et al.*, Phys. Rev. D **72**, 033003 (2005); K. Hagiwara, N. Okamura and K. i. Senda, Phys. Lett. B **637**, 266 (2006).
- [33] O. Mena, S. Palomares-Ruiz and S. Pascoli, Phys. Rev. D **73**, 073007 (2006).
- [34] T. Kajita *et al.*, arXiv:hep-ph/0609286.
- [35] J. Burguet-Castell *et al.*, Nucl. Phys. B **646**, 301 (2002);
- [36] P. Huber, M. Lindner and W. Winter, Nucl. Phys. B **654**, 3 (2003).
- [37] H. Minakata, H. Nunokawa and S. J. Parke, Phys. Rev. D **68**, 013010 (2003).
- [38] V. Barger, D. Marfatia and K. Whisnant, Phys. Lett. B **560**, 75 (2003).
- [39] K. Whisnant, J. M. Yang and B. L. Young, Phys. Rev. D **67**, 013004 (2003); P. Huber *et al.*, Nucl. Phys. B **665**, 487 (2003); P. Huber *et al.*, Phys. Rev. D **70**, 073014 (2004); A. Donini, E. Fernández-Martínez and S. Rigolin, Phys. Lett. B **621**, 276 (2005).

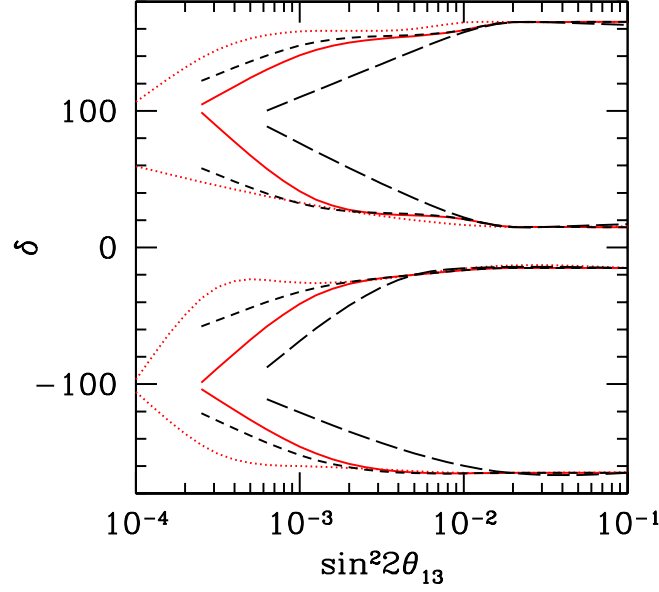


FIG. 11: 99% *CL* *CP* Violation extraction (2 d.o.f) assuming that the far detector is located at a distance of 1480. The solid (dotted) red curves depict the results assuming 3×10^{22} Kton-decays (1×10^{23} Kton-decays) without backgrounds. The long-dashed (short-dashed) black curves depict the results assuming 3×10^{22} Kton-decays (1×10^{23} Kton-decays) with a background level of 10^{-3} .

- [40] O. Mena and S. J. Parke, Phys. Rev. D **70**, 093011 (2004).
- [41] P. Huber, M. Maltoni and T. Schwetz, Phys. Rev. D **71**, 053006 (2005).
- [42] A. Blondel *et al.*, Acta Phys. Polon. B **37**, 2077 (2006). A. Blondel hep-ph/0606111.
- [43] O. Mena, H. Nunokawa and S. J. Parke, Phys. Rev. D **75**, 033002 (2007). O. Mena, hep-ph/0609031.
- [44] International scoping study of a future Neutrino Factory and super-beam facility Report, in preparation.
- [45] D. Ayres *et al.*, hep-ex/0503053.
- [46] J. Hylen *et al.*, FERMILAB-TM-2018, (1997).
- [47] K. S. McFarland, Eur. Phys. J. A **24S2**, 187 (2005).
- [48] P. Baringer *et al.* [D0 Collaboration], Nucl. Instrum. Meth. A **469**, 295 (2001).
- [49] Ambrosio *et al.*, Fermilab-TM-2149, June, 2001.
- [50] V. Kashikhin, private communication
- [51] A. Cervera-Villanueva, J. J. Gomez-Cadenas and J. A. Hernando, Nucl. Instrum. Meth. A **534**, 180 (2004).
- [52] D. Casper, Nucl. Phys. Proc. Suppl. **112**, 161 (2002).
- [53] A. Bueno, M. Campanelli and A. Rubbia, Nucl. Phys. B **589** 577 (2000).
- [54] A. Donini *et al* Nucl. Phys. B **743**, 41 (2006).
- [55] A. de Gouvea, J. Jenkins and B. Kayser, Phys. Rev. D **71**, 113009 (2005) [arXiv:hep-ph/0503079].
- [56] A. de Gouvea and W. Winter, Phys. Rev. D **73**, 033003 (2006) [arXiv:hep-ph/0509359].
- [57] H. Minakata, H. Nunokawa, S. J. Parke and R. Zukanovich Funchal, Phys. Rev. D **74**, 053008 (2006) [arXiv:hep-ph/0607284].